American Journal of Applied Chemistry
2024, Vol. 12, No. 6, pp. 135-148
https://doi.org/10.11648/j.ajac.20241206.12

Research Article

Investigation on the Properties of Methyl 4-(((1-H benzo[d]imidazol-2-yl) methyl)thio)methyl)Benzoate on Aluminum Corrosion in Acidic Environment

Rokia Hadja Toure[1], Aphouet Aurelie Koffi[1, *], Mougo Andre Tigori[2], Paulin Marius Niamien[1]

[1]Laboratory of Constitution and Reaction of Matter, Training and Research Unit of Sciences of Structure, Matter and Technology, Felix Houphouet Boigny University, Abidjan, Ivory Coast

[2]Laboratory of Environmental Sciences and Technologies, Training and Research Unit of Environment, Jean Lorougnon Guede University, Daloa, Ivory Coast

Abstract

Organic inhibitors are crucial for preserving metals from corrosion in acidic environments. In this regard, the methyl 4-(((1-H benzo[d]imidazol-2-yl)methyl)thio)methyl)benzoate (M-41HBI-2MTMB) was synthesized and investigated as an eco-friendly inhibitor for aluminum in a molar nitric acid solution (1 M HNO_3). The gravimetric technique was used to study the inhibitory properties of the molecule, and the density functional theory (DFT) was conducted to elucidate the corrosion inhibition mechanism. The experimental data indicated that M-41HBI-2MTMB reduced the corrosion of the metal with a significant inhibition efficiency. The corrosion inhibition increased with an increase in the concentration of the molecule, reaching an efficiency of 98.5% at a concentration of 5.10^{-3} M, and a temperature of 298 K. Adsorption isotherms and thermodynamic parameters were studied to elucidate the interactions between M-41HBI-2MTMB and the metal surface. The inhibitor adsorbed spontaneously onto the aluminum surface following the Villamil model (modified Langmuir isotherm). Additionally, the Gibbs free energy less than - 40 $kJ.mol^{-1}$ and the negative value of the enthalpy of adsorption suggested mixed-type adsorption with a predominance of physical interactions. The theoretical findings of DFT calculations revealed a positive fraction of electrons transferred ($\Delta N = 0.247$ *eV*), a high value of the electrophilicity index ($\omega = 3.807$ *eV*) as well as a low energy gap ($\Delta E = 4.478$ *eV*) showing favorable interactions of M-41HBI-2MTMB with its environment. The active sites of the molecule were highlighted at the level of carbon atoms, and a corrosion inhibition mechanism was proposed.

Keywords

Aluminum, Methyl 4-(((1-H benzo[d]imidazol-2-yl)methyl)thio)methyl)benzoate (M-41HBI-2MTMB), Gravimetric Measurement, Density Functional Theory (DFT)

[*]Corresponding author: koffiaphouet@yahoo.fr (Aphouet Aurelie Koffi)

Received: 6 November 2024; **Accepted:** 19 November 2024; **Published:** 12 December 2024

1. Introduction

Industries commonly use acid solutions to seal and clean metal systems [1]. These industrial processes ensure the smooth running and efficiency of the plant. However, corrosion occurs during these processes, and aluminum structures are not spared [2]. Beyond the huge economic losses, corrosion causes environmental degradation and risks human health. Corrosion of materials is, therefore, a significant global problem [3, 4].

Appropriate techniques can be used to protect against corrosion and its effects, such as applying potential corrosion inhibitors and protective coatings [5]. The commonly used method to mitigate corrosion of metals in an aqueous environment is the addition of inhibitors, classified into organic and inorganic compounds [6-8]. For example, inorganic inhibitors such as chromate, molybdate, and vanadate ions exhibit excellent corrosion protection capability. However, these compounds are hazardous and harmful [5, 9].

When selecting inhibitors, efforts are made to protect humans and the environment. Thus, non-toxic and biodegradable organic compounds are preferred [10-12]. Many organic inhibitors have been studied to reduce the corrosion rate of aluminum structures, including nitroimidazopyridinehydrazone derivatives [13], theophylline [14], and thiophene [6]. These molecules protect the metal by adsorbing physically or chemically on the substrate surface. The inhibitor's capacity to get adsorbed depends on the molecule's structure (heteroatoms and π bonds), the type of electrolyte, the excess surface charge of the metal, and the working conditions [15, 16].

It is in this imperative of research on green inhibitors that this work was carried out. The inhibitory properties of methyl 4-(((1-H benzo [d] imidazole-2-yl) methyl) thio) methyl) benzoate on the corrosion of aluminum in 1 M HNO_3 solution was investigated. The molecule of interest belongs to the benzimidazole derivatives. It contains heteroatoms (N, O, and S) and aromatic rings that can facilitate its interactions with the metal surface because the adsorption process is essential in the inhibitory effectiveness of an organic compound [17-19].

Several authors have reported the inhibitory properties of benzimidazole derivatives in acidic environments. For instance, Timoudan et al. [20] studied the corrosion inhibition properties of (1H-benzimidazol-2-yl)methanethiol (LF1) and 1-dodecyl-2-((dodecylthio)methyl)-1H benzimidazole (LF2) in 1 M hydrochloric acid solution by numerous methods. The inhibition rate reached 88.2% and 95.4% for LF1 and LF2, respectively. Likewise, Guendouz and al. [21] investigated the inhibitory properties of two newly synthesized benzimidazole derivatives, namely 1-(cyclohex-1-en-1-yl)-3-[(3-phenyl-1,2-oxazol-5-yl)methyl] -2,3-dihydro-1H-1,3-benzodiazol-2-one (Benz1) and 1-(cyclohex-1-en-1-yl)-3-[(3-phenyl-4, 5-dihydro-1,2-oxazol-5-yl)methyl]-2,3-dihydro-1H-1,3-benz odiazol-2-one (Benz2). In this study, Benz1 and Benz2 were evaluated as corrosion inhibitors using both experimental methods and computational approaches.

Many other benzimidazole derivatives have attracted much interest in metal corrosion protection [22-29]. These molecules were synthesized and studied in extremely aggressive environments, such as acidic solutions as well as in sodium hydroxide and salt media. Also, the metals tested are diverse. All these benzimidazole derivatives exhibited good inhibitory performances.

This study aims to synthesize and investigate the anticorrosion behavior of methyl 4-(((1-H benzo [d] imidazole-2-yl) methyl) thio) methyl) benzoate using experimental and theoretical techniques. On the one hand, the corrosion rate of aluminum and the inhibition efficiency of the molecule studied were evaluated using gravimetric measurements. On the other hand, the corrosion inhibition mechanism was elucidated through thermodynamic parameters and Density Functional Theory (DFT) calculations.

2. Materials and Methods

2.1. Aluminium Samples and Electrolyte Medium

Gravimetric tests were performed using high-purity (99.6%) aluminum rods cut into 1 cm lengths. Each aluminum sample was subjected to polishing with abrasive paper, washing with distilled water, and degreasing with an acetone solution; then oven drying at 353 K for 10 minutes. Subsequently, each sample was weighed and immersed in 50 mL of 1 M HNO_3 without and with M-41HBI-2MTMB in a concentration range from 0.001 to 5 mM. After one hour, the sample was removed from the solution and rinsed thoroughly with distilled water. This is followed by oven drying and re-weighing. Each test was repeated at least three times to check the reproducibility of the results.

2.2. Inhibitor Synthesis

The synthesis of methyl 4-((((1-H benzo [d] imidazole-2-yl) methyl) thio) methyl) benzoate followed the procedure outlined by Souleymane Coulibaly et al [30]. It was carried out in two reaction steps, summarized in Figure 1. First, isothiouronium-1-H-benzimidazole salt is formed by adding 7g of ortho phenylenediamine to 7g of 2-chloroacetic acid in 60 ml of 4 N hydrochloric acid solution. Then, the formed salt was added to methyl-4-bromomethyl benzoate in a sodium hydroxide solution.

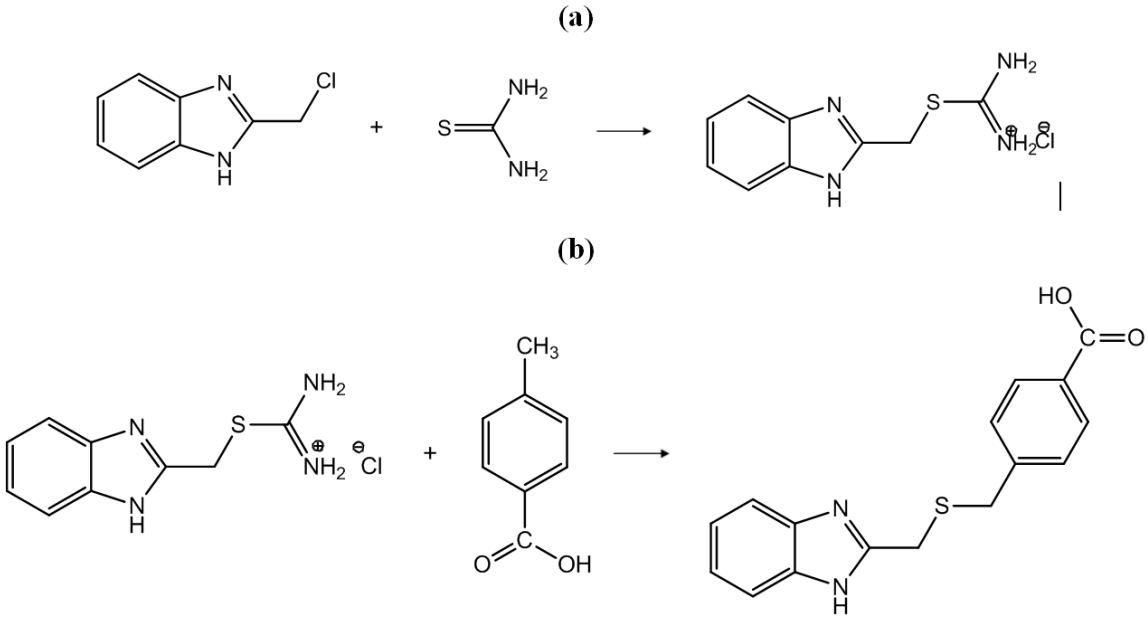

Figure 1. *Synthesis of methyl 4-(((1-H benzo [d] imidazole-2-yl) methyl) thio) methyl) benzoate.*

2.3. Gravimetry Method

The corrosion rate W (g. cm^{-2}. h^{-1}) of the sample and the inhibition efficiency E (%) of the M-41HBI-2MTMB molecule were determined using the equations below:

$$W = \frac{\Delta m}{S \times t} \quad (1)$$

$$E = \frac{W_0 - W}{W_0} \times 100 \quad (2)$$

Here Δm represents the mass loss (g); S denotes the total area of the specimen (cm^2); t represents the immersion time (h); W_0 and W are the corrosion rates without and with inhibitor, respectively.

2.4. Density Functional Theory Calculations

To explore the reactivity of the molecule under investigation, quantum chemistry calculations were carried out employing the Gaussian 09W software package at DFT/B3LYP method with a 6-311G++ (d, p) basis set [31]. Before calculations, the molecule was drawn, and the structure was pre-optimized using GaussView 5.0.8. Then, the descriptors of the global reactivity, namely the energy of the highest occupied molecular orbital (E_{HOMO}) and the lowest unoccupied molecular orbital (E_{LUMO}), as well as the dipole moment (μ) and the total energy (E_T) were obtained. Subsequently, the electronegativity (χ), the electrophilicity index (ω), the fraction of electrons transferred (ΔN), and the energy gap (ΔE) were determined using the following equations:

$$\chi = -\frac{(E_{HOMO} + E_{LUMO})}{2} \quad (3)$$

$$\omega = \frac{\chi^2}{2\eta} \quad (4)$$

$$\Delta N = \frac{\phi_{Al} - \chi_{inh}}{2(\eta_{Al} + \eta_{inh})} \quad (5)$$

$$\Delta E = E_{LUMO} - E_{HOMO} \quad (6)$$

Where $\eta_{Al} = 0$ eV and η_{inh} are the hardness of aluminium and the inhibitor, respectively. The work function $\phi_{Al} = 4.28$ eV was used instead because the electronegativity χ_{Al} is conceptually wrong here [32].

To further understand the reactivity of the M-41HBI-2MTMB molecule, the Fukui functions (f_k^+ and f_k^-) used to specify the sites prone to electrophilic and nucleophilic attack are determined by the equations above:

$$f_k^+ = q_k(N+1) - q_k(N) \quad (7)$$

$$f_k^- = q_k(N) - q_k(N-1) \quad (8)$$

In these expressions, $q_k(N)$, $q_k(N+1)$ and $q_k(N-1)$ are the Mulliken charges of the atom k in the neutral, anionic, and cationic forms, respectively.

3. Results and Discussions

3.1. Gravimetric Results

3.1.1. Effect of M-41HBI-2MTMB on the Aluminium Corrosion

Figure 2 below shows the corrosion rate of aluminum investigated in 1M HNO_3 solution. This figure indicates that the aluminum sample dissolves in the corrosive medium. Dissolution increases particularly with rising temperature. Indeed, thermal agitations facilitate the movements of the reactants in the solution [33, 34]. However, by adding M-41HBI-2MTMB in the corrosive environment, the corrosion rate decreased significantly.

The effectiveness of this inhibitor is evaluated as shown in Figure 3. The inhibition rate of the molecule increases from 65.27 % to 98.51 % at 298 K, which means that the inhibitory barrier becomes increasingly dense with the inhibitor concentration. It is reported that in an acidic environment, an organic species exerts its inhibitory action by getting adsorbed on the surface of the metal to be protected [17-19]. The decrease observed when the temperature reaches 338 K is due to the desorption of inhibitory species from the surface of the metal [35]. Despite a weaker adsorption process of M-41HBI-2MTMB species at higher temperatures, the metal is effectively protected with an inhibitory efficiency of 74.3% at a concentration of 5.10^{-3} M.

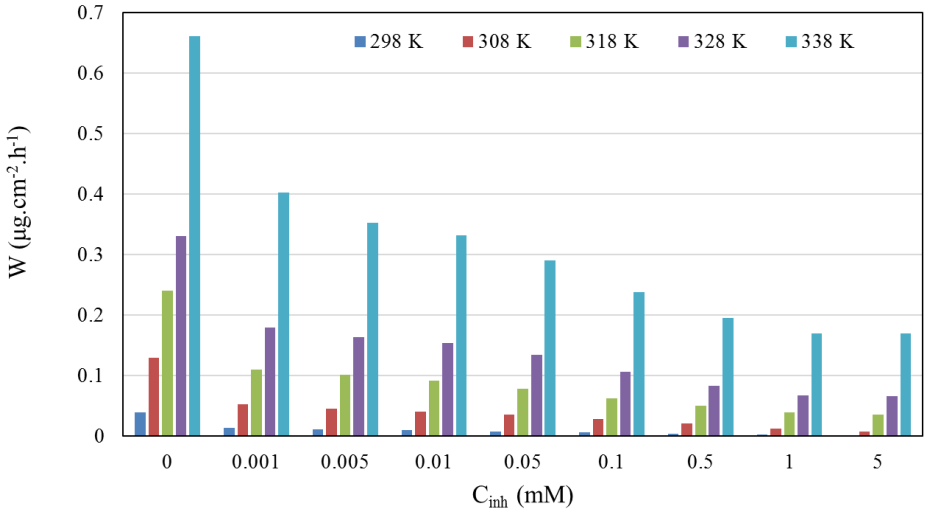

Figure 2. *Corrosion rate of aluminium in 1M HNO_3 environment versus M-41HBI-2MTMB concentration, at different temperatures.*

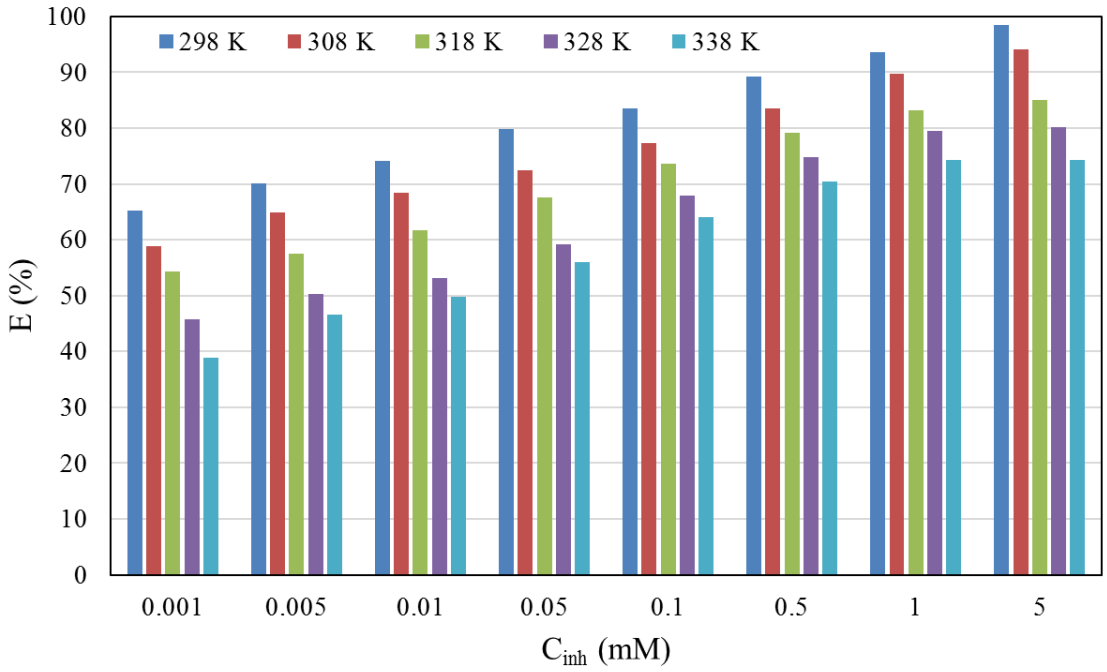

Figure 3. *Inhibition efficiency versus M-41HBI-2MTMB concentration, at different temperatures.*

3.1.2. Adsorption Isotherms and Thermodynamic Parameters

The study of isotherms is crucial because it is necessary to elucidate the nature of the interactions between an inhibitor and the metal surface. Thus, the modeling of adsorption was carried out using the surface coverage (θ) through various models. The appropriate model that best fits the surface coverage is given by the coefficients of determination closest to unity. The Langmuir isotherm (Figure 4) presents the highest fitting line coefficients (Table 1), but the slopes do not equal unity. Therefore, the modified Langmuir isotherm (Villamil isotherm [36]) of equation (9) below better describes the adsorption of M-41HBI-2MTMB species onto the aluminum surface in 1M HNO_3 medium, suggesting the presence of interactions between adsorbed species, a non-uniform distribution of adsorption sites on the metal surface, and the formed multilayer adsorption [37].

$$\frac{C_{inh}}{\theta} = \frac{n}{K_{ads}} + n\,C_{inh} \tag{9}$$

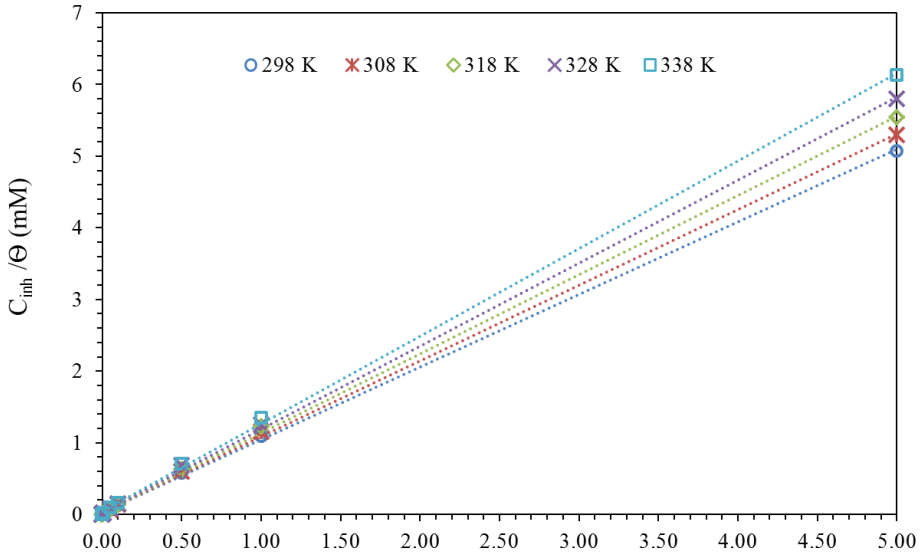

Figure 4. *Langmuir isotherm applied to the adsorption of M-41HBI-2MTMB molecule on the aluminum surface in 1 M HNO_3 solution.*

Table 1. *Langmuir isotherm parameters for M-41HBI-2MTMB on the aluminum surface.*

T (K)	Equation	R^2	K_{ads} (10^{-3} M)
298	$C_{inh}/\theta = 1.0127\,C_{inh} + 0.026$	0.9997	38950
308	$C_{inh}/\theta = 1.0570\,C_{inh} + 0.028$	0.9996	37750
318	$C_{inh}/\theta = 1.1052\,C_{inh} + 0.033$	0.9994	33491
328	$C_{inh}/\theta = 1.1570\,C_{inh} + 0.035$	0.9996	33057
338	$C_{inh}/\theta = 1.2223\,C_{inh} + 0.039$	0.9995	31341

The key parameters including the adsorption free energy (ΔG_{ads}), the adsorption enthalpy (ΔH_{ads}) and the adsorption entropy (ΔS_{ads}) are determined through the following equations:

$$\Delta G_{ads} = -RTLn(55.5\,K_{ads}) \tag{10}$$

$$\ln K_{ads} = \frac{-\Delta H_{ads}}{RT} + \frac{\Delta S_{ads}}{R} \tag{11}$$

55.5 represents the water's molar concentration, R is the universal gas constant (8.31 $J.mol^{-1}.K^{-1}$) and T denotes the absolute temperature (K).

From the results (Table 2), the negative values of ΔG_{ads} highlight the spontaneous adsorption process of M-41HBI-2MTMB on the aluminium surface. Furthermore, the values vary between – 40 and – 20 $kJ.mol^{-1}$ assuming both chemisorption and physisorption processes [19, 38]. The negative sign of ΔH_{ads} indicates an exothermic process as-

sociated with the physical adsorption type of M-41HBI-2MTMB [39, 40]. From the positive value of the entropy, it could be concluded that an increase in disorder accompanies the adsorption of the inhibitory species due to the desorption of water molecules previously adsorbed on the aluminum surface [35].

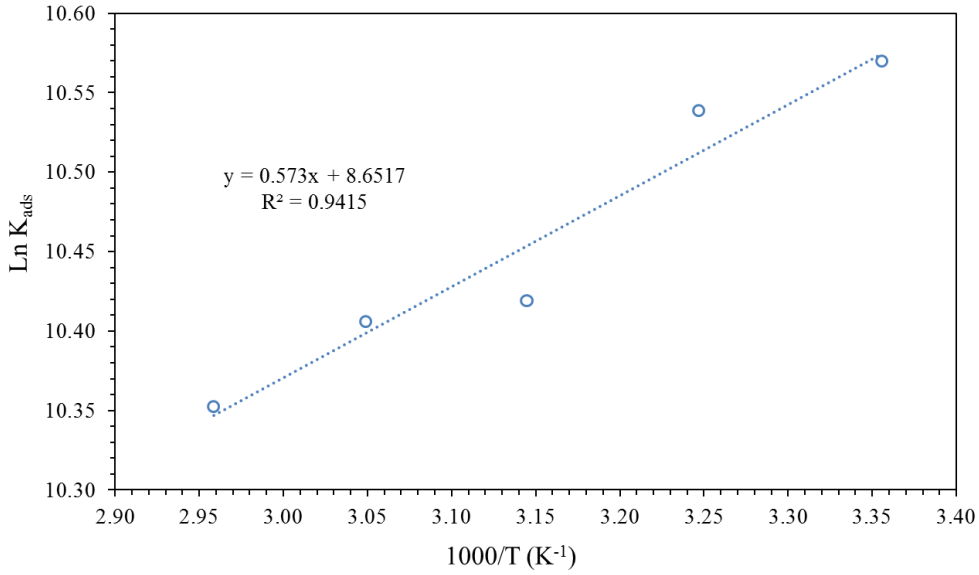

Figure 5. *Plot of* $Ln\ K_{ads}$ *versus* T *of M-41HBI-2MTMB on the aluminum surface.*

Table 2. *Adsorption parameters of M-41HBI-2MTMB on the aluminium surface.*

T (K)	$-\Delta G_{ads}$ (kJ.mol^{-1})	$-\Delta H_{ads}$ (kJ.mol^{-1})	ΔS_{ads} (J.mol^{-1}.K^{-1})
298	36.122		
308	37.254		
318	38.147	4.762	47.869
328	39.311		
338	40.360		

The adsorption phenomenon was also investigated by plotting $log\ W$ and $log\ (W/T)$ versus $1000/T$ using linear forms of the Arrhenius relation (Equation 12) and the transition state relation (Equation 13). In these relations, the parameters sought are the energy (E_a^*), the enthalpy variation (ΔH_a^*) and the entropy variation (ΔS_a^*) of activation.

$$\log W = -\frac{E_a^*}{2.303\ RT} + \log k_0 \qquad (12)$$

$$\log \frac{W}{T} = -\frac{\Delta H_a^*}{2.303\ RT} + \frac{\Delta S_a^*}{2.303\ R} + \log \frac{R}{Nh} \qquad (13)$$

Figure 6 and Table 3 represent the results obtained. The literature reports that upon the addition of an inhibitor in an acidic medium, an increase in E_a^* is associated with physisorption. Still, the decrease in activation energy is attributed to chemisorption [39-41]. Remarkably, the higher values of E_a^* in the inhibited acidic solutions could be related to a physical barrier formed by the adsorption of the M-41HBI-2MTMB species. The ΔH_a^* values are positive, indicating that the dissolution of aluminim in this corrosive environment is a heat-consuming process. Similarly, the ΔS_a^* values are positive meaning that the corrosion of aluminim is accompanied by an increase in disorder due to a dissociative mechanism of the activated complex [42]. Furthermore, increasing the concentration of M-41HBI-2MTMB promotes the increase of E_a^*, ΔH_a^* and ΔS_a^*. The adsorption of this inhibitor improves the inhibitory barrier and contributes to the disorder.

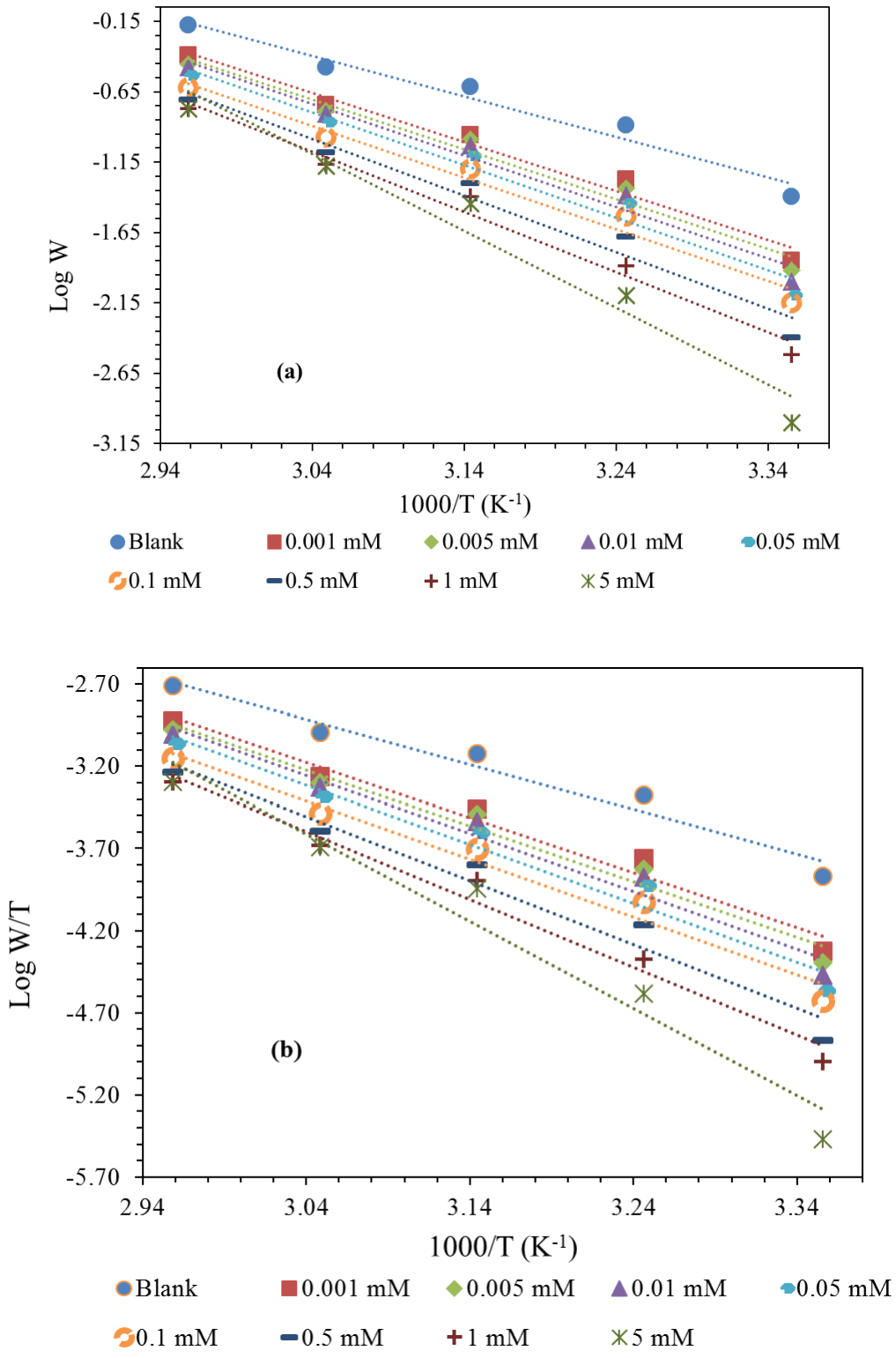

Figure 6. *Plots of (a) $log\ W$ and (b) $log\ (W/T)$ versus $1000/T$ of aluminium in 1 M HNO_3 without and with M-41HBI-2MTMB.*

Table 3. *Activation parameters of aluminium surface in 1M HNO_3 medium without and with M-41HBI-2MTMB.*

C_{inh} (mM)	E_a^* (kJ.mol^{-1})	ΔH_a^* (kJ.mol^{-1})	ΔS_a^* (J.mol^{-1}K^{-1})
Blank	55.03	52.40	301.08
0.001	66.74	64.10	331.59

C_{inh} (mM)	E_a^* (kJ.mol^{-1})	ΔH_a^* (kJ.mol^{-1})	ΔS_a^* (J.mol^{-1}K^{-1})
0.005	67.60	64.97	333.33
0.01	70.09	67.46	340.30
0.05	71.58	68.95	343.69
0.1	70.24	67.60	337.79
0.5	77.05	74.42	356.66
1	81.84	79.20	369.54
5	104.42	101.78	437.82

3.2. Theoretical Study and Inhibition Mechanism

3.2.1. Quantum Calculations

The adsorption mechanism of the molecule under investigation was further discussed with quantum chemistry. Thus, the global and local reactivity parameters of the M-41HBI-2MTMB molecule were determined using Density Functional Theory (DFT) calculations. The analysis of the defined parameters informs us about the molecule's active sites and capability to share electrons with its environment. The optimized molecule and the frontier orbitals are depicted in Figure 7. From the figure, it is noticed that the HOMO density is distributed over the benzimidazole ring, and the LUMO electron density is concentrated around the carboxybenzene. Consequently, the active sites of the inhibitor could be located at any atom.

(a)

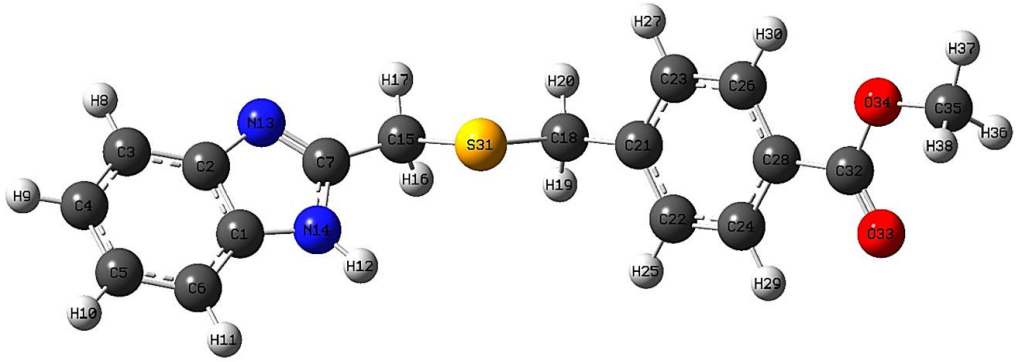

(b)

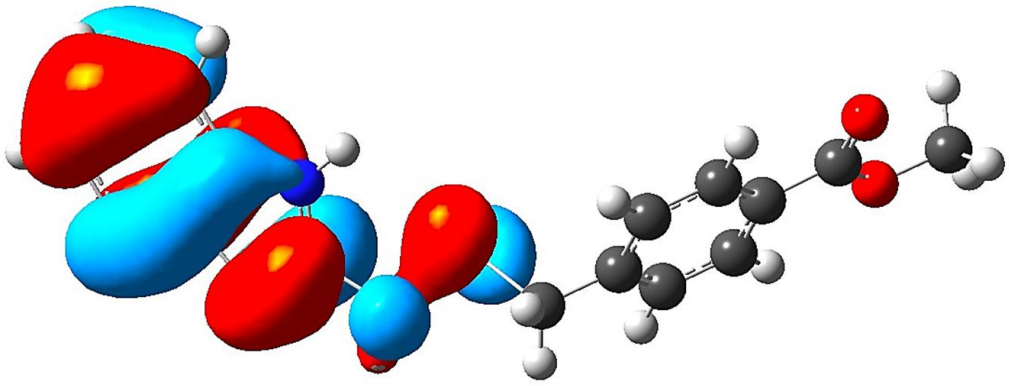

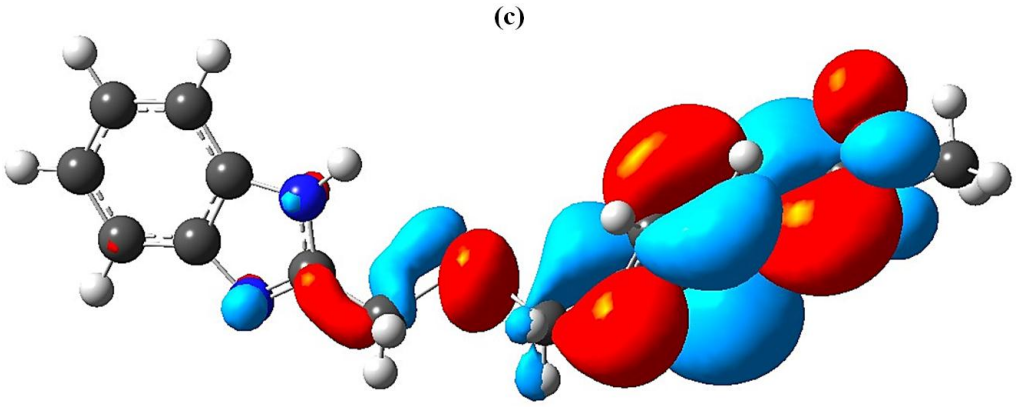

Figure 7. *Optimized structure and HOMO and LUMO orbitals of M-41HBI-2MTMB.*

The energies of the frontier orbitals (E_{HOMO} and E_{LUMO}) as well as the fraction of electrons transferred (ΔN) and the electrophilicity index (ω) are indicated in Table 4. The global descriptors of the molecule studied are consistent with the literature values [31, 32, 43-45]. E_{HOMO} is high characterizing the molecule's tendency to donate electrons, while E_{LUMO} is low demonstrating its ability to accept electrons. Therefore, M-41HBI-2MTMB can interact with its environment which is supported by a low energy gap (ΔE = *4.478 eV*). Furthermore, the high value of the electrophilicity index (ω = *3.807 eV*) confirms the electrophilic nature of the studied molecule, and the fraction of electrons transferred (ΔN = *0.247 eV*) indicates that M-41HBI-2MTMB donates electrons to the surface of aluminum. In sum, the global descriptors suggest favorable interactions between the molecule and its environment.

Table 4. *Global reactivity descriptors of M-41HBI-2MTMB.*

E_{HOMO} (eV)	E_{LUMO} (eV)	ΔE (eV)	μ (D)	E_T (ua)	χ (eV)	η (eV)	S (eV^{-1})	ω (eV)	ΔN
-6.368	-1.890	4.478	1.997	-1315.889	4.129	2.239	0.447	3.807	0.247

Table 5 provides the index dual that specifies the electrophilic and nucleophilic attack sites involved in these interactions. This descriptor is determined from the Fukui functions as:

$$\Delta f_k = f_k^+ - f_k^- \quad (14)$$

Here, f_k^+ and f_k^- are the nucleophilic and electrophilic Fukui functions.

According to the literature [46-48], the zones sensitive to nucleophilic attack are highlighted by the highest values of the dual descriptor. In contrast, the lowest values of Δf_k underscore the sites prone to electrophilic attack. In this study, the C(15) and C(18) carbon atoms exhibit the highest values of Δf_k and may serve as the nucleophilic attack sites. On the contrary, the lowest dual index identifies C(7) and C(21) as potential electrophilic attack sites.

Table 5. *Mulliken charges, Fukui functions and dual descriptor of pertinent atoms of M-41HBI-2MTMB.*

Atom N°	$q_k(N-1)$	$q_k(N)$	$q_k(N+1)$	f_k^+	f_k^-	Δf_k
C(1)	0.534	0.502	0.615	0.113	-0.032	0.145
C(2)	0.443	0.232	0.021	-0.211	-0.211	0.000
C(3)	-0.377	-0.374	-0.222	0.152	0.003	0.149
C(4)	-0.465	-0.417	-0.302	0.115	0.048	0.067
C(5)	-0.208	-0.250	-0.223	0.027	-0.042	0.069

Atom N°	$q_k(N-1)$	$q_k(N)$	$q_k(N+1)$	f_k^+	f_k^-	Δf_k
C(6)	-0.653	-0.622	-0.389	0.233	0.031	0.202
C(7)	-0.110	0.597	-0.025	-0.622	0.707	-1.329
N(13)	-0.094	-0.081	0.043	0.124	0.013	0.111
N(14)	-0.061	-0.112	-0.079	0.033	-0.051	0.084
C(15)	-0.449	-1.017	-0.719	0.298	-0.568	0.866
C(18)	-0.201	-1.12	-0.831	0.289	-0.919	1.208
C(21)	0.998	1.543	1.016	-0.527	0.545	-1.072
C(22)	-0.695	-0.502	-0.507	-0.005	0.193	-0.198
C(23)	-0.568	-0.512	-0.488	0.024	0.056	-0.032
C(24)	-0.485	-0.347	-0.383	-0.036	0.138	-0.174
C(26)	-0.566	-0.322	-0.355	-0.033	0.244	-0.277
C(28)	0.594	0.524	0.593	0.069	-0.070	0.139
S(31)	-0.459	-0.000	0.398	0.398	0.459	-0.061
C(32)	-0.086	-0.167	-0.184	-0.017	-0.081	0.064
O(33)	-0.327	-0.266	-0.244	0.022	0.061	-0.039
O(34)	-0.140	-0.119	-0.120	-0.001	0.021	-0.022
C(35)	-0.234	-0.216	-0.221	-0.005	0.018	-0.023

3.2.2. Proposed Inhibition Mechanism

Literature reported that corrosion inhibition in an acidic environment occurs through adsorption of the inhibitor onto the metal surface [20, 22, 46, 48]. The adsorption process includes physical or chemical interactions, or a combination of the two, influenced by several factors such as the metal's surface charge and the inhibitor's chemical structure. Several mechanisms could be proposed.

When exposed to an acidic environment, the aluminum surface takes on a positive charge. The chloride ions present in the solution are then adsorbed onto the positively charged metal surface. Besides, in an acidic environment, an organic molecule undergoes protonation. Subsequently, interactions occur between the protonated inhibitor and previously adsorbed chloride ions [49]. In this work, the most favorable site in M-41HBI-2MTMB for protonation is the N(13) atom. The protonated inhibitor (M-41HBI-2MTMBH$^+$) can be physically adsorbed onto the aluminum surface as shown in Figure 8. M-41HBI-2MTMBH$^+$ could also be chemically adsorbed onto the metal surface. The presence of the aromatic ring facilitates this chemisorption which could notably occur at the level of C(7) and C(21) atoms.

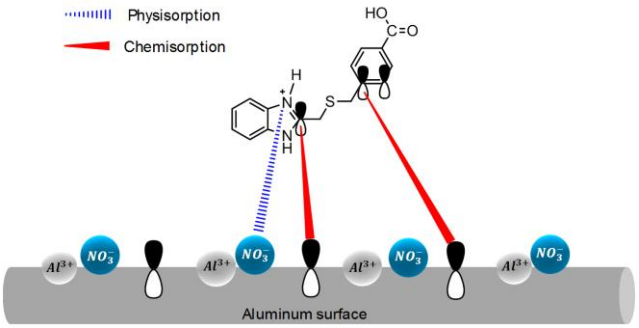

Figure 8. *Adsorption process of the protonated inhibitor on the aluminum surface.*

It is also possible that M-41HBI-2MTMB formed metal complexes with Al^{3+} released in the acidic solution [50]. These cations contribute to the inhibition of the aluminum surface by physical adsorption. Moreover, protonated M-41HBI-2MTMB can compete with H^+ ions at the cathodic sites on the aluminum surface, by accepting electrons formed during the metal oxidation [51]. This mechanism agrees with DFT results as certified by the positive ΔN parameter. In addition, the inhibitor can cover a larger metal surface contributing to high inhibition efficiency.

4. Conclusions

The molecule methyl 4-(((1-H benzo[d]imidazol-2-yl)methyl)thio)methyl)benzoate was explored as a corrosion inhibitor of aluminum in a 1 M HNO_3 solution using a combination of gravimetric analysis to examine the compound's effectiveness and the DFT calculations to provide additional insights into the molecular behavior.

Experimental results revealed that adding this molecule to the acidic medium significantly reduced the corrosion of aluminum, thus demonstrating its inhibitory properties. The inhibition efficiency increased with higher concentrations, from 10^{-6} M to 5.10^{-3} M, reaching up to 98.5 % at a temperature of 298 K. The adsorption of methyl 4-(((1-H benzo[d]imidazol-2-yl)methyl)thio)methyl)benzoate followed the Villamil isotherm, suggesting repulsive interactions and formation of multiple layers on the metal surface. Analysis of thermodynamic parameters suggested a predominance of physisorption.

Density Functional Theory (DFT) calculations highlighted distinct distributions of the HOMO and LUMO electron densities of the molecule. Theoretical results also suggested a high reactivity due to a low energy gap. The active sites identified by the Fukui functions are C(15) and C(18) for electrophilic attack, C(7), and C(21) for nucleophilic attack. Additionally, electrons are transferred from the methyl 4-(((1-H benzo[d]imidazol-2-yl)methyl)thio)methyl)benzoate molecule to the metal surface with a positive fraction of electron transfer ($\Delta N = 0.247$ eV). Experimental and theoretical approaches are consistent with the inhibitory behavior of the molecule and the mechanism underlying its adsorption mode.

Abbreviations

DFT	Density Functional Theory
HOMO	Highest Occupied Molecular Orbital
LUMO	Lowest Unoccupied Molecular Orbital
M-41HBI-2MTMB	Methyl 4-(((1-H benzo[d]imidazol-2-yl) methyl)thio)methyl)Benzoate

Author contributions

Rokia Hadja Touré Investigation, Validation, Formal Analysis, Methodology, Software.

Aphouet Aurelie Koffi: Writing – original draft, Data curation, Writing – review & editing, Formal Analysis, Methodology.

Mougo Andr éTigori: Writing – original draft, Data curation, Writing – review & editing, Formal Analysis, Methodology.

Paulin Marius Niamien: Conceptualization, Supervision, Data curation, Validation, Methodology, Visualization.

Funding

No funding was received during the preparation of this manuscript.

Conflicts of Interest

The authors declare no conflicts of interest.

References

[1] Kumari, A., Jha, M. K., Lee, J.-c., Singh, R.P. Clean process for recovery of metals and recycling of acid from the leach liquor of PCBs. *Journal of Cleaner Production*. 2016, 112(5), 4826-4834. https://doi.org/10.1016/j.jclepro.2015.08.018

[2] Zhu, T., Yu, Y. Y. Q., Xiang, H., Liu, G., Dai, X., Liao, R. Enhanced corrosion resistance of slippery liquid infused porous aluminum surfaces prepared by anodizing in simulated marine atmosphere. *Materials Chemistry and Physics*. 2023, 306, 128073. https://doi.org/10.1016/j.matchemphys.2023.128073

[3] Ahmed, Al-A., Wan, N. R. W. I., Waleed, K. Al-A. Sustainable corrosion Inhibitors: A key step towards environmentally responsible corrosion control. *Ain Shams Engineering Journal*. 2024, 15, 102672. https://doi.org/10.1016/j.asej.2024.102672

[4] Kania H., Corrosion and Anticorrosion of Alloys/Metals: The Important Global Issue. *Coatings*. 2023, 13(2), 216. https://doi.org/10.3390/coatings13020216

[5] Zamindar, S., Mandal, S., Murmu, M., Banerjee, P. Unveiling the future of steel corrosion inhibition: a revolutionary sustainable odyssey with a special emphasis on N^+-containing ionic liquids through cutting-edge innovations. *Materials Advances*. 2024, 5, 4563–4600. https://doi.org/10.1039/d4ma00156g

[6] Arrousse, N., Fernine, Y., Al-Zaqri, N., Boshaala, A., Ech-chihbi, E., Salim, R., Hajjaji, F. E., Alami, A., Touhami, M. E., Taleb, M. Thiophene derivatives as corrosion inhibitors for 2024-T3 aluminum alloy in hydrochloric acid medium. *RSC Advances*. 2022, 12(17), 10321-10335. https://doi.org/10.1039/d2ra00185c

[7] Chahid, A., Chafi, M., Essahli, M., Alrashdi, A. A., Lgaz, H. Exploring the efficacy of Congo Red dye as a corrosion inhibitor for aluminum in HCl solution: An interdisciplinary study with RSM modeling and theoretical simulations. *Arabian Journal of Chemistry*. 2024, 17(7), 105810. https://doi.org/10.1016/j.arabjc.2024.105810

[8] Boughoues, Y., Benamira, M., Messaadia, L., Ribouh, N. Adsorption and corrosion inhibition performance of some environmentally friendly organic inhibitors for mild steel in HCl solution via experimental and theoretical study. *Colloids and Surfaces A: Physicochemical and Engineering*. 2020, 593, 124610. https://doi.org/10.1016/j.colsurfa.2020.124610

[9] Milošev, I., Pavlovčič, T., Tomšič, M. Molybdate and vanadate ions as corrosion inhibitors for clad aluminium alloy 2024-T3. *Electrochimica Acta*. 2024, 504, 144893. https://doi.org/10.1016/j.electacta.2024.144893

[10] Wang, Q., Li, H. Study on anodic oxidation of 2099 aluminum lithium alloy and sealing treatment in environmentally friendly solutions. *International Journal of Electrochemical Science*. 2023, 18(7): 100186.

[11] Žaklina, Z., TasićMarija, B., Mihajlović, P., Radovanović, M. B., Simonović, A. T., Antonijević, M. M. Experimental and theoretical studies of paracetamol as a copper corrosion inhibitor. *Journal of Molecular Liquids*. 2021, 327, 114817. https://doi.org/10.1016/j.molliq.2020.114817

[12] El-Hajjaji, F., Merimi, I., Messali, M., Obaid, R.J., Salim, R., Taleb, M., Hammouti, B. Experimental and quantum studies of newly synthesized pyridazinium derivatives on mild steel in hydrochloric acid medium. *Materials Today: Proceedings*. 2019, 13(3), 822-831. https://doi.org/10.1016/j.matpr.2019.04.045

[13] Tigori, M. A., Adingra, K. F., Koné, A., M'Bouillé, C., Sissouma, D., Niamien. P. M. Comparative Study of Two Nitro imidazo pyridine hydrazone Derivatives Inhibition Action for Aluminum Corrosion in 2M HCl: Experimental and Theoretical Insights. *Chemical Science Review and Letters*. 2024, 13 (49), 7-20.

[14] Beda R.H.B., Tigori, M.A., Diabaté, D. and Niamien, P.M., Anticorrosive Properties of Theophylline on Aluminium Corrosion in 1 M HCl: Experimental, and Computational Assessment of Iodide Ions Synergistic Effect. *Current Physical Chemistry*. 2021, 11(3), 227-242.

[15] Wang L., Wang H., Seyeux A., Zanna S., Pailleret A., Nesic S., Marcus P., Adsorption mechanism of quaternary ammonium corrosion inhibitor on carbon steel surface using ToF-SIMS and XPS, *Corrosion Science*. 2023, 213(1): 110952. https://doi.org/10.1016/j.corsci.2022.110952

[16] Betti N., Al Amiery A.A., Al Azzawi W.K., Isahak W.N.R.W., Corrosion inhibition properties of schiff base derivative against mild steel in HCl environment complemented with DFT investigations. *Scientific Reports*. 2023, 13, 8979. https://doi.org/10.1038/s41598-023-36064-w

[17] Solmaz, R., Salcı, A., Dursun, Y. A., Kardaş, G. A comprehensive study on the adsorption, corrosion inhibition efficiency and stability of acriflavine on mild steel in 1 M HCl solution. *Colloids and Surfaces A: Physicochemical and Engineering Aspects*. 2023, 674, 131908. https://doi.org/10.1016/j.colsurfa.2023.131908

[18] Annon, I. A., Alamiery, A. S. A. A. A., Al-Azzawi, W. K., Isahak, W. N. R. W., Hanoon, M. M., Kadhum, A. A. H., Corrosion inhibition of mild steel in hydrochloric acid environment using thiadiazole derivative: Weight loss, thermodynamics, adsorption and computational investigations. *South African Journal of Chemical Engineering*. 2022, 41, 244–252. https://doi.org/10.1016/j.sajce.2022.06.011

[19] Ghaderi, M., Ahmad Ramazani, S.A., Kordzadeh, A., Mahdavian, M., Alibakhshi, E., Ghaderi, A. Corrosion inhibition of a novel antihistamine based compound for mild steel in hydrochloric acid solution: experimental and computational studies. *Scientific Reports*. 2022, 12, 13450. https://doi.org/10.1038/s41598-022-17589-y

[20] Timoudan, N., Al-Gorair, A. S., Foujji, L. E., Warad, I., Safi, Z., Dikici, B., Benhiba, F., Qaiss, A. E. K., Bouhfid, R., Bentiss, F., Al-Juaid, S. S., Abdallah, M., Zarrouk, A. Corrosion inhibition performance of benzimidazole derivatives for protection of carbon steel in hydrochloric acid solution. *RSC Advances*. 2024, 14, 30295–30316. https://doi.org/10.1039/d4ra05070c

[21] Guendouz, A., Ettahiri, W., Adardour, M., Lazrak, J., Assiri, E. H. E., Taleb, A., Hammouti, B., Rais, Z., Baouid, A., Taleb, M. New Benzimidazole derivatives as efficient organic inhibitors of mild steel corrosion in hydrochloric acid medium: Electrochemical, SEM/EDX, MC, and DFT studies. *Journal of Molecular Structure*. 2025, 1321(3), 139901. https://doi.org/10.1016/j.molstruc.2024.139901

[22] Marinescu, M. Recent advances in the use of benzimidazoles as corrosion inhibitors. *BMC Chemistry*. 2019, 13, 136. https://doi.org/10.1186/s13065-019-0655-y

[23] Nagy, H. A. E., Tamany, E. H. E., Ashour, H., El-Azabawy, O. E., Zaki, Elsayed, G., Elsaeed, S. M. Polymeric Ionic Liquids Based on Benzimidazole Derivatives as Corrosion Inhibitors for X‑65 Carbon Steel Deterioration in Acidic Aqueous Medium: Hydrogen Evolution and Adsorption Studies. *ACS Omega*. 2020, 5(47), 30577–30586. https://doi.org/10.1021/acsomega.0c04505

[24] Ran, B., Wei, Z., Yu, S., Zhi, H., Yan, S., Cai, S., Wen, L., Fan, B., Wang, J., Wang, K., Luo, X. The study on corrosion inhibition effect of 2-Phenylbenzimidazole for X70 steel in HCl solution at 308K. *International Journal of Electrochemical Science*. 2023, 18, 100032. https://doi.org/10.1016/j.ijoes.2023.100032

[25] Yousif, Q. A, Fadel, Z., Abuelela, A. M, Alosaimi, E. H., Melhi, S., Bedair, M. A. Insight into the corrosion mitigation performance of three novel benzimidazole derivatives of amino acids for carbon steel (X56) in 1 M HCl solution. *RSC Advances*. 2023, 13(19), 13094–13119. https://doi.org/10.1039/d3ra01837g

[26] Khormali, A., Ahmadi, S. Experimental and modeling analysis on the performance of 2-mercaptobenzimidazole corrosion inhibitor in hydrochloric acid solution during acidizing in the petroleum industry. *Journal of Petroleum Exploration and Production Technology*. 2023, 13, 2217–2235. https://doi.org/10.1007/s13202-023-01675-6

[27] Liu, Q., Xiao, W., Ge, P., Long, W., Gao, S., Liu, X., Chen, Y. Corrosion Inhibition Effect of 2-Chloro-1-(4-fluorobenzyl) benzimidazole on Copper in 0.5 M H_2SO_4 solution. *International Journal of Electrochemical Science*. 2022, 17, 221299. https://doi.org/10.20964/2022.12.110

[28] Zhang, J., Li, H. 2-(2-chlorophenyl)-1H-Benzimidazole as a New Corrosion Inhibitor for Copper in Sulfuric Acid. *International Journal of Electrochemical Science*. 2020, 15, 5362 – 5372. https://doi.org/10.20964/2020.06.63

[29] Rouifi, Z., Rbaa, M., Abousale, A. S., Benhiba, F., Laabaissi, T., Oudda, H., Lakhrissi, B., Guenbour, A., Warad, I., Zarrou, A. Synthesis, characterization and corrosion inhibition potential of newly benzimidazole derivatives: Combining theoretical and experimental study. *Surfaces and Interfaces*. 2020, 18, 100442. https://doi.org/10.1016/j.surfin.2020.100442

[30] Coulibaly, S., Coulibali, S., Bamba, F., Achi, P.-A., Kouadio, F. K., Evrard A., Anéé, A. Synthesis and effect of N-alkylation on antibacterial activity of 2-(Benzylthio) methyl-1H-benzimidazole derivatives. *GSC Biological and Pharmaceutical Sciences*. 2022, 20(03), 272–279. https://doi.org/10.30574/gscbps.2022.20.3.0370

[31] Rokia, T. H., Tigori, M. A., Koffi, A. A., Niamien, P. M., Exploring the Anticorrosion Performance of 2-(((4-Chlorobenzyl) Thiol) Methyl)-1H-Benzo[d]imidazole on Aluminum in 1 M HNO_3. *Journal of Scientific Research*. 2024, 16 (3), 899-915. https://dx.doi.org/10.3329/jsr.v16i3.72318

[32] Bine, F.K., Tasheh, S.N., Nkungli, N.K., Ghogomu, J.N. Corrosion inhibition of aluminum in gas and acid media by some chalcone-based N-(3-Aminopropyl) imidazoles: TD-DFT-based FMO, conceptual DFT, QTAIM and EDA studies. *Computational Chemistry*. 2021, 9, 37-63. https://doi.org/10.4236/cc.2021.91003

[33] Husaini, M., Yunusa, U., Ibrahim, H.A., Usman, B., Ibrahim, M. B. Corrosion inhibition of aluminium in phosphoric acid solution using glutaraldehyde as inhibitor. *Algerian Journal of Chemical Engineering*. 2020, 01, 12–21. https://doi.org/10.5281/zenodo.3986577

[34] Ajiwe, V. I. E., Ejike, C. E. Inhibitory Action of Methanol Leaf Extract of Irvingia Gabonensis on the Corrosion of Mild Steel in H2SO4. *American Journal of Applied Chemistry*. 2019, 7(2), 72-79. https://doi.org/10.11648/j.ajac.20190702.15

[35] Al Amiery, A. A., Mohamad, A. B., Kadhum, A. A. H., Shaker, L. M., Isahak, W. N. R. W., Takriff, M. S. Experimental and theoretical study on the corrosion inhibition of mild steel by nonanedioic acid derivative in hydrochloric acid solution. *Scientific Reports*. 2022, 12: 4705. https://doi.org/10.1038/s41598-022-08146-8

[36] Andoor, P. A., Okeoma, K. B., Mbamara, U. S. Adsorption and thermodynamic studies of the corrosion inhibition effect of Rosmarinus officinalis L. leaves on aluminium alloy in 0.25 M HCl and effect of an external magnetic field. *International Journal of Physical Sciences*. 2021, 16(2), 79-95. https://doi.org/10.5897/IJPS2021.4945

[37] Alahiane, M., Oukhrib, R., Albrimi, Y. A., Oualid, H. A., Bourzi, H., Akbour, R. A., Assabbane, A., Nahlé, A., Hamdan M. Experimental and theoretical investigations of benzoic acid derivatives as corrosion inhibitors for AISI 316 stainless steel in hydrochloric acid medium: DFT and Monte Carlo simulations on the Fe (110) surface. *RSC Advances*. 2020, 10, 41137–41153.

[38] Go, L.C., Depan, D., Holmes, W. E., Gallo, A., Knierim, K., Bertrand T., Hernandez R., Kinetic and thermodynamic analyses of the corrosion inhibition of synthetic extracellular polymeric substances. *PeerJ Materials Science*. 2020, 2:e4. https://doi.org/10.7717/peerj-matsci.4

[39] Gómez-Sánchez, G., Olivares-Xometl, O., Arellanes-Lozada, P., Likhanova, N. V., Lijanova, I. V., Arriola-Morales, J., Díaz-Jiménez, V., López-Rodríguez, J. Temperature Effect on the Corrosion Inhibition of Carbon Steel by Polymeric Ionic Liquids in Acid Medium. *International Journal of Molecular Sciences*. 2023, 24, 6291. https://doi.org/10.3390/ijms24076291

[40] Nsude, O. P., Orie, K. J. Thermodynamic and Adsorption Analysis of Corrosion Inhibition of Mild Steel in 0.5M HCl Medium via Ethanol Extracts of Phyllanthus mellerianus. *American Journal of Applied Chemistry*. 2022, 10(3), 67-75. https://doi.org/10.11648/j.ajac.20221003.12

[41] Budnyak, T. M., Błachnio, M., Slabon, A., Jaworski, A., Tertykh, V. A., Deryło-Marczewska, A., Marczewski, A. W. Chitosan Deposited onto Fumed Silica Surface as Sustainable Hybrid Biosorbent for Acid Orange 8 Dye Capture: Effect of Temperature in Adsorption Equilibrium and Kinetics. *Journal of Physical Chemistry C*. 2020, 124, 15312−15323. https://doi.org/10.1021/acs.jpcc.0c04205

[42] Ogunyemi, B. T., Latona, D. F., Ayinde, A. A., Adejoro, I. A. Theoretical investigation to corrosion inhibition efficiency of some chloroquine derivatives using density functional theory. *Advanced Journal of Chemistry-Section A*. 2020, 3, 485–492. https://doi.org/10.33945/SAMI/AJCA.2020.4.10

[43] Esan, T. O., Oyeneyin, O. E., Olanipekun, A. D., Ipinloju, N. Corrosion Inhibitive Potentials of Some Amino Acid Derivatives of 1,4-Naphthoquinone−DFT Calculations. *Advanced Journal of Chemistry-Section A*. 2022, 5(4), 263-270. https://doi.org/10.22034/ajca.2022.353882.1321

[44] Akbas, E., Ruzgar, A. Synthesis, characterization, and DFT calculation of some new pyrimidine derivatives and theoretical studies on the corrosion inhibition performance. *Iranian Journal of Chemistry and Chemical Engineering*. 2022, 41, 1643 – 1656. https://doi.org/10.30492/ijcce.2021.521495.4479

[45] Hanoon, M. M., Gbashi, Z. A., Al-Amiery, A. A., Kadhim, A., Kadhum, A. A. H., Takriff, M. S. Study of corrosion behavior of N'-acetyl-4-pyrrol-1-ylbenzohydrazide for low carbon steel in the acid environment: experimental, adsorption mechanism, surface investigation, and DFT studies. *Progress in Color, Colorants and Coatings*. 2022, 15, 133-141.

[46] Oluwatoba, E. O., Nathanael, D. O., Nureni, I. E. B. A., Abiodun, V. E. Investigation of the corrosion inhibition potentials of some 2-(4-(substituted) arylidene)-1H-indene-1,3-dione derivatives: density functional theory and molecular dynamics simulation. *Beni-Suef University Journal of Basic and Applied Sciences*. 2022, 11, 132. https://doi.org/10.1186/s43088-022-00313-0

[47] Tigori, M. A., Kouyaté, A., Kouakou, V., Niamien, P. M., Trokourey, A. Inhibition Performance of Some Sulfonylurea on Copper Corrosion in Nitric Acid Solution Evaluated Theoretically by DFT Calculations. *Open Journal of Physical Chemistry*. 2020, 10, 139-157. https://doi.org/10.4236/ojpc.2020.103008

[48] Gadow, H. S., Alayyafi, A. A., Farghaly, T. A., Eldesoky, A. M. Corrosion inhibition properties of perimidin-10-one derivatives for steel reinforcement in acidic environments: Experimental and theoretical insights. *International Journal of Electrochemical Science*. 2024, 19(5), 100545. https://doi.org/10.1016/j.ijoes.2024.100545

[49] Nouteza, A. M., Pengou, M., Ngamy, J. P. M., Hou, P., Tchekwagep, J. J. K., et al. Synthesis and Performance of a New and Simple Schiff Base Structure for Corrosion Inhibition of C38 steel in 1 M HCl Solution: Experimental Studies and DFT Investigation. *Modern Chemistry*. 2024, 12(1), 6-27. https://doi.org/10.11648/j.mc.20241201.12

[50] Fouda, A. S., Abdel-Wahed, H. M., Atia, M. F., El-Hossiany, A. Novel porphyrin derivatives as corrosion inhibitors for stainless steel 304 in acidic environment: synthesis, electrochemical and quantum calculation studies. *Scientific Reports*. 2023, 13, 17593, https://doi.org/10.1038/s41598-023-44873-2

[51] Gurjar, S., Sharma, S. K., Sharma, A., Ratnani, S. Pyridazinium based ionic liquids as green corrosion inhibitors: An overview. *Electrochemical Science Advances*. 2022, 2: e2100110. https://doi.org/10.1002/elsa.202100110